

Aluminum nanowires: Influence of work hardening on conductance histograms

I. K. Yanson,^{1,2} O. I. Shklyarevskii,^{1,3} J. M. van Ruitenbeek,² and S. Speller³

¹*B.I. Verkin Institute for Low Temperature Physics and Engineering, National Academy of Sciences of Ukraine, 47, Lenin Avenue, 61103 Kharkov, Ukraine*

²*Kamerlingh Onnes Laboratorium, Universiteit Leiden, Postbus 9504, 2300 RA Leiden, The Netherlands*

³*Institute for Molecules and Materials, University of Nijmegen, Toernooiveld 1, 6525 ED Nijmegen, The Netherlands*

(Received 13 July 2007; published 22 January 2008)

Conductance histograms of work-hardened Al show a series up to 11 equidistant peaks with a period of 1.15 ± 0.02 of the quantum conductance unit $G_0 = 2e^2/h$. Assuming that the peaks originate from atomic discreteness, this agrees with the value of $1.16 G_0$ per atom obtained in numerical calculations by Hasmy *et al.* [Phys. Rev. B **72**, 245405 (2005)].

DOI: [10.1103/PhysRevB.77.033411](https://doi.org/10.1103/PhysRevB.77.033411)

PACS number(s): 73.40.Jn, 73.63.-b, 68.65.La

Stability and self-organization phenomena in metallic nanowires (NWs) are controlled by an intimate combination of the quantum nature of the conduction electrons and the atomic-scale surface energy (for a review, see Ref. 1). At the scale of single atoms, Au, Pt, and Ir spontaneously form into chains.²⁻⁴ For larger diameters, more complex morphologies including spiral and helical multishell structures (often referred to as “weird wires”) were predicted^{5,6} and eventually observed in high-resolution transmission electron microscopy (TEM).⁷⁻⁹

Electronic shell effects can stabilize and therefore favor certain geometries. Independent series of stable nanowire diameters with periodicities proportional to the square root of the conductance \sqrt{G} were observed for the free-electron-like alkali metals^{10,11} and the noble metals.¹²⁻¹⁴ Although these NWs were not imaged as by TEM, their stability was deduced from the statistical analysis of frequently occurring stable conductance values during breaking of the contacts.

With increasing NW diameter, the contribution of the surface energy becomes more important and stable configurations are governed by the atomic packing. This gives rise to an atomic shell filling series and the crossover between electronic and atomic shell structure has been observed in the conductance of alkali and noble metal nanowires^{13,14,21} as a change in the regular period on the scale \sqrt{G} . Atomic shell filling has been observed in TEM as exceptionally long and stable wires,¹⁵⁻¹⁷ predominantly along $\langle 110 \rangle$.

During last two years, the effects of pseudoelastic deformation and shape memory in nanowires of the simple fcc metals (Ag, Cu) has drawn considerable attention.^{18,19} These effects occur through the formation of defect-free twins during the $\langle 100 \rangle$ to $\langle 110 \rangle / \{111\}$ reorientation process. One can expect the emerging of stable configurations during a cycle of contraction and elongation of the NW. However, such configurations will be nanowire specific and depend on NW diameter, crystallographic orientation, existence of defects, etc. An example of striking repetitiveness of the conductance during the cyclical deformation (without breaking) of a long Au neck at 4.2 K was presented already in Ref. 20.

Recently, we have reported the observation of a new series of structures periodic in G , rather than \sqrt{G} , in conductance histograms of work-hardened gold.²² We suggested that heavy work hardening of the starting wire results in a high

density of intercrystalline boundaries and leads to the texture of the most dense crystal planes $[111]$, $[100]$, and $[110]$ being perpendicular to the nanowire axis. The distances Δg between the maxima in conductance histograms correspond to the changes in the smallest cross section of densest planes by an integer number of atoms. The increment in conductance is then expected to scale as $\Delta g_{111} / \Delta g_{100} / \Delta g_{110} \cong 0.87 / 1 / 1.41$ based on the size of the atomic unit cells. The Fourier transform of the data revealed three “frequencies” at a close ratio: $\sim 0.8, 1.1,$ and $1.4 G_0^{-1}$. The mechanical properties of nanocrystalline materials (including NWs²³) differ drastically from those of single crystals. In the case of work-hardened materials, the mobility of atoms at grain boundaries may be high enough to adjust the local orientation of the grains on each side of the contact along one of the principal crystallographic axes.

Numerical simulations of conductance histograms for gold using a parametrized tight-binding approach were performed by Dreher *et al.*²⁴ They demonstrated for the main crystallographic orientations a series of peaks in histograms for the minimal cross sections that is related to the atomic discreteness. However, they found that this periodic structure in the minimal cross section was not reflected in conductance histograms in their calculations.

Here, we report the observation of atomic-size oscillations for aluminum nanocontacts. The extension of this effect, previously observed for noble metals, to trivalent Al is of principal significance. One may anticipate that changing the nanowire cross section by a single atom for noble metals results in a change in conductance by approximately one quantum.²⁵ In Al, three valence electrons give rise to three quantum channels: a highly transmissive channel with sp_z character and two low transmissive channels with a p_x, p_y character.²⁶⁻²⁸ The most unexpected result of our experiments is that the incremental conductance between adjacent maxima in conductance histograms of work-hardened Al is again close to one quantum conductance for up to about 11 oscillations (see below). In the case of Al, we can no longer apply quasiclassical considerations as we did for Au and have to use a quantum mechanical approach. Such approach was elaborated by Hasmy *et al.*,^{29,30} who performed an embedded atom molecular dynamics method coupled with full quantum calculations of electron transport using a procedure

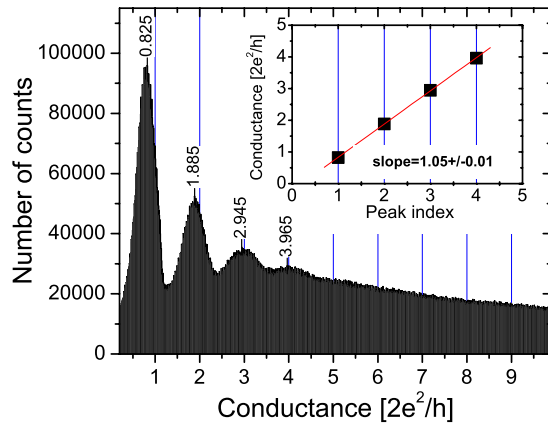


FIG. 1. (Color online) Conductance histogram for annealed Al. The bias voltage was 80 mV and the histogram was constructed from 11 900 breaking traces, at $T=4.2$ K. With about 1000 points per digitized curve, the total number of data points in the histogram is of order 10^7 . Inset: the position of the maxima in the conductance histogram versus the peak index, giving a slope of $1.05 \pm 0.01 G_0$.

based on the *ab initio* Gaussian embedded-cluster method.³¹ The results reveal a statistically linear relationship between the conductance and the number of aluminum atoms in the contact cross section with the slope equal to $1.16 G_0$.

Conductance histograms are constructed from a large number of contact-breaking traces and show the probability for observing a given conductance value G . While for chemically inert gold conductance histograms of reasonable quality can be measured in air using very simple table-top devices,³² this is much less obvious for chemically active aluminum, although some results have recently been reported.³³ The main problem is that the hardness of aluminum oxide exceeds by far that of Al (400 compared to 8 at absolute hardness scale). The direct electrical contact between the electrodes can be established only by a “hard indenting” procedure³⁴ causing substantial damage to the lattice. An obvious solution to this problem is to employ the mechanically controllable break junction technique described in detail in Ref. 1. In our experiments, the notched aluminum wire is broken under cryogenic vacuum conditions at 4.2 K exposing two electrodes with atomically clean surfaces. Accurately controlled indentation-retraction cycles can be obtained through the action of a piezoelectric element. On rare occasions ($\leq 5\%$), featureless or ill-reproducible histograms were observed with a small number of maxima positioned at significantly lower G as compared to the rest of the data. Possibly, this is caused by the break of the work-hardened wire occurring along an oxidized microcrack or grain boundary.

For well-annealed³⁶ Al, one typically observes several peaks in the histogram near $G=nG_0$, with $n=1, 2, 3, 4$ (Fig. 1). One more peak is sometimes found near $5 G_0$, but in most cases only peaks up to $3 G_0$ are visible. Although a contribution of conductance quantization effects cannot be excluded completely, the main reason of the appearance of the peaks is the discreteness of the atomic structure of the contacts.^{1,35} The first peak results from single-atom contacts and higher peaks are due to stable atomic arrangements involving more atoms in the contact cross section (see Fig. 3 in Ref. 30).

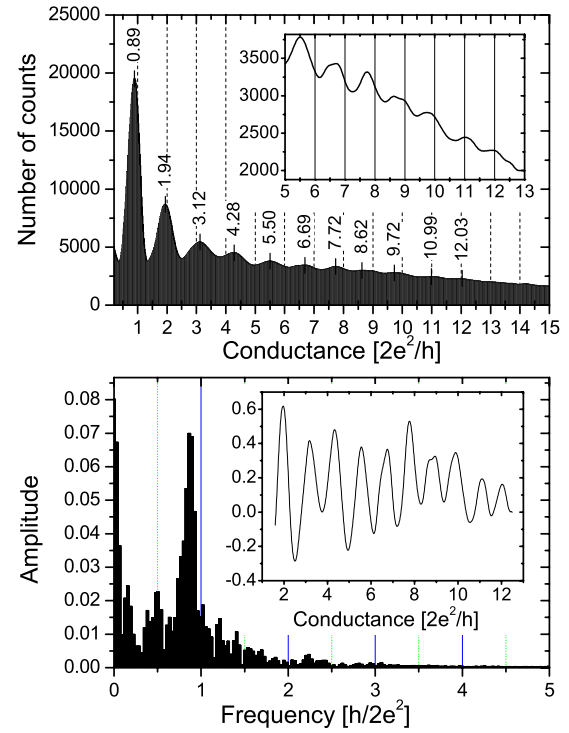


FIG. 2. (Color online) Upper panel: histogram exhibiting one of the highest numbers of peaks for work-hardened Al. Bias voltage, 80 mV; number of traces, 21 030; $T=4.2$ K. The structure of the histograms is insensitive to the variation of the bias voltage in the range from 10 to 100 mV. Inset: magnified portion of the histogram between $G_0=5$ and 13. Lower panel: Fourier spectrum of the conductance histogram presented above after rescaling, as shown in the inset (see text). The peak at $0.87 G_0^{-1}$ corresponds to an average histogram peak spacing of $1.15 G_0$.

In our experiments we used two types of Al wires. Part of the measurements was done with commercial “temper hard” samples.³⁷ Practically the same results were obtained by work hardening of annealed wires. To this end, we pulled wires through a series of sapphire dies, reducing the diameter from 250 to 100 μm . In both cases, it was possible to observe a structure periodic in G having up to 11 oscillations in the conductance range from 0 to $13 G_0$ (Fig. 2, upper panel). The position of maxima in the conductance histograms and their relative intensity were accurately reproduced for different samples.

The oscillating part of the histogram is presented in the inset to the lower panel of Fig. 2. It was obtained by subtracting the nearly linear background and by normalizing through division by the enveloping curve. The Fourier spectrum of this rescaled histogram shows a peak at the “frequency” $0.87 \pm 0.01 G_0^{-1}$ (lower panel in Fig. 2). Assuming that the oscillations result from atomic discreteness in analogy to those observed²² for Au, this number is very close to the slope $0.86 G_0^{-1}$ obtained in numerical simulations for nanowires with a $\langle 111 \rangle$ oriented axis.³⁰

The histogram presented above was obtained for conductance traces recorded while breaking the contact. One can also take histograms for traces of contact closing, which we refer to as return histograms. We measured direct and return

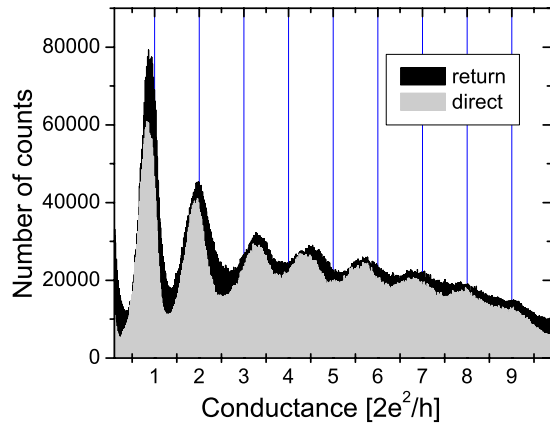


FIG. 3. (Color online) Direct conductance histogram (obtained for breaking contacts, gray) versus return histogram (closing contacts, black) for the same cycle of measurement.

histograms for work-hardened Al by applying an isosceles triangle ramp voltage to the piezodriver and separating data for the pulling and pushing parts of the cycle. Surprisingly, these histograms are practically equivalent (Fig. 3). This is quite different from our observations for work-hardened gold, where the number of the atomic-scale oscillations was greatly reduced in the return histograms and the electronic shell structure was observed in 40% of the latter.²²

Conductance histograms for work-hardened Au invariably show a clear “beating” pattern in the peak intensities related to the existence of several closely separated periodicities. In contrast for Al histograms with the largest number of peaks (10–11), we observed only a smooth decrease of the enveloping curve and a single frequency in the Fourier spectra around $0.87 G_0$. In search for different periods, we paid attention to histograms with lower numbers of peaks (Fig. 4). One notices kinks in the envelope curve for the histogram maxima (inset in Fig. 4). Although these irregularities may indicate contributions from the various axis orientations, the magnitude of the effect is rather small and the number of peaks in the histogram is not sufficient for more detailed analysis.

Assuming the $\langle 111 \rangle$ periodicity is due to atom-size oscillation effects similar to our previous results on Au wires,²² we can estimate a Fermi wave vector k_F in Al for effective free electrons propagating along the (111) plane per one atom change of (111) cross section. Using the Sharvin formula, we obtain a value of $k_F = 1.55 \times 10^{10} \text{ m}^{-1}$ for the effective momentum in Al.

The picture emerging from our experiments on Au²² and

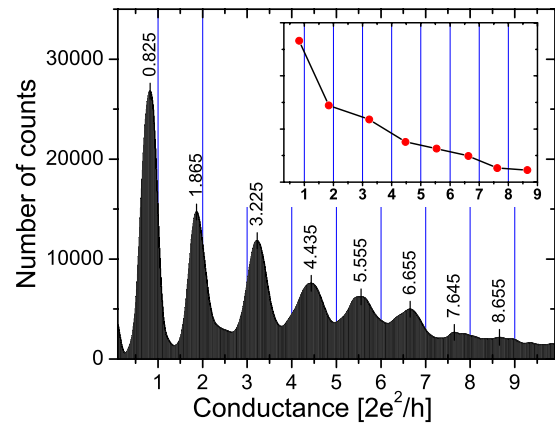


FIG. 4. (Color online) Upper panel: typical conductance histogram for work-hardened Al with eight maxima. Inset: enveloping curve for histogram. Bias voltage, 99 mV; number of curves, 11 196; $T=4.2$ K.

more specifically for Al is as follows. For single crystalline necks with the highest atomic packing in the transverse crystal plane [like the (111) plane], not only are the Al atoms stacked at definite positions in the nodes of the lattice but also their orbitals are oriented in the same way. Hence, three valence electrons contribute to the conductance with a contribution that scales with the number of atoms. This property is at the heart of the observed linear dependencies of contact conductance on the numbers of atoms in the smallest cross section of the nanowire. These atomic arrangements are associated with transient minima of the lattice free energy leading to maxima on conductance histograms.

Summarizing, we observed a periodic structure in the conductance histograms of work-hardened Al wires, which agrees with a series of stable wire cross sections given by integer numbers of atoms, combined with a conductance per atom as calculated by Hasmy *et al.*³⁰ for the (111) orientation of the nanowire axis. The experimentally observed peak in the Fourier transform at $0.87 G_0^{-1}$ is very close to the calculated value of $0.86 G_0^{-1}$. We believe that this periodic structure is due to the same mechanism suggested for Au atomic-scale oscillations observed earlier.²²

Part of this work was supported by the Nanotechnology network in the Netherlands NanoNed, the Dutch nanotechnology programme of the Ministry of Economic Affairs, the Stichting voor Fundamenteel Onderzoek der Materie (FOM) which is financially supported by the Netherlands Organization for Scientific research (NWO), and the NANO-programme of Ukraine. O.I.S. wishes to acknowledge the FOM for a visitor’s grant.

¹N. Agrait, A. Levy Yeyati, and J. M. van Ruitenbeek, *Phys. Rep.* **377**, 81 (2003).

²H. Ohnishi, Y. Kondo, and K. Takayanagi, *Nature (London)* **395**, 780 (1998).

³A. I. Yanson, G. Rubio Bollinger, H. E. van den Brom, N. Agrait,

and J. M. van Ruitenbeek, *Nature (London)* **395**, 783 (1998).

⁴R. H. M. Smit, C. Untiedt, A. I. Yanson, and J. M. van Ruitenbeek, *Phys. Rev. Lett.* **87**, 266102 (2001).

⁵O. Gulseren, F. Ercolessi, and E. Tosatti, *Phys. Rev. Lett.* **80**, 3775 (1998).

- ⁶E. Tosatti and S. Prestipino, *Science* **289**, 561 (2000).
- ⁷Y. Kondo and K. Takayanagi, *Science* **289**, 606 (2000).
- ⁸Y. Oshima, H. Koizumi, K. Mouri, H. Hirayama, K. Takayanagi, and Y. Kondo, *Phys. Rev. B* **65**, 121401(R) (2002).
- ⁹Y. Oshima, A. Onga, and K. Takayanagi, *Phys. Rev. Lett.* **91**, 205503 (2003).
- ¹⁰A. I. Yanson, I. K. Yanson, and J. M. van Ruitenbeek, *Nature (London)* **400**, 144 (1999).
- ¹¹A. I. Yanson, I. K. Yanson, and J. M. van Ruitenbeek, *Phys. Rev. Lett.* **84**, 5832 (2000).
- ¹²E. Medina, M. Diaz, N. Leon, C. Guerrero, A. Hasmy, P. A. Serena, and J. L. Costa-Kramer, *Phys. Rev. Lett.* **91**, 026802 (2003).
- ¹³A. I. Mares, A. F. Otte, L. G. Soukiassian, R. H. M. Smit, and J. M. van Ruitenbeek, *Phys. Rev. B* **70**, 073401 (2004).
- ¹⁴A. I. Mares and J. M. van Ruitenbeek, *Phys. Rev. B* **72**, 205402 (2005).
- ¹⁵Y. Kondo and K. Takayanagi, *Phys. Rev. Lett.* **79**, 3455 (1997).
- ¹⁶T. Kizuka, *Phys. Rev. Lett.* **81**, 4448 (1998).
- ¹⁷V. Rodrigues, T. Fuhrer, and D. Ugarte, *Phys. Rev. Lett.* **85**, 4124 (2000).
- ¹⁸H. S. Park, K. Gall, and J. A. Zimmerman, *Phys. Rev. Lett.* **95**, 255504 (2005).
- ¹⁹W. Liang and M. Zhou, *Phys. Rev. B* **73**, 115409 (2006).
- ²⁰C. Untiedt, G. Rubio, S. Vieira, and N. Agraït, *Phys. Rev. B* **56**, 2154 (1997).
- ²¹A. I. Yanson, I. K. Yanson, and J. M. van Ruitenbeek, *Phys. Rev. Lett.* **87**, 216805 (2001).
- ²²I. K. Yanson, O. I. Shklyarevskii, Sz. Csonka, H. van Kempen, S. Speller, A. I. Yanson, and J. M. van Ruitenbeek, *Phys. Rev. Lett.* **95**, 256806 (2005).
- ²³A. Bietsch and B. Michel, *Appl. Phys. Lett.* **80**, 3346 (2002).
- ²⁴M. Dreher, F. Pauly, J. Heurich, J. C. Cuevas, E. Scheer, and P. Nielaba, *Phys. Rev. B* **72**, 075435 (2005).
- ²⁵E. Scheer, W. Belzig, Y. Naveh, M. H. Devoret, D. Esteve, and C. Urbina, *Phys. Rev. Lett.* **86**, 284 (2001).
- ²⁶J. C. Cuevas, A. L. Yeyati, and A. Martín-Rodero, *Phys. Rev. Lett.* **80**, 1066 (1998).
- ²⁷J. C. Cuevas, A. Levy Yeyati, A. Martín-Rodero, G. R. Bollinger, C. Untiedt, and N. Agraït, *Phys. Rev. Lett.* **81**, 2990 (1998).
- ²⁸E. Scheer, P. Joyez, D. Esteve, C. Urbina, and M. H. Devoret, *Phys. Rev. Lett.* **78**, 3535 (1997).
- ²⁹A. Hasmy, E. Medina, and P. A. Serena, *Phys. Rev. Lett.* **86**, 5574 (2001).
- ³⁰A. Hasmy, A. J. Perez-Jimenez, J. J. Palacios, P. Garcia-Mochales, J. L. Costa-Kramer, M. Diaz, E. Medina, and P. A. Serena, *Phys. Rev. B* **72**, 245405 (2005).
- ³¹J. J. Palacios, A. J. Perez-Jimenez, E. Louis, E. SanFabian, and J. A. Verges, *Phys. Rev. B* **66**, 035322 (2002).
- ³²K. Hansen, E. Lægsgaard, I. Stensgaard, and F. Besenbacher, *Phys. Rev. B* **56**, 2208 (1997).
- ³³A. I. Mares, D. F. Urban, J. Bürki, H. Grabert, C. A. Stafford, and J. M. van Ruitenbeek, *Nanotechnology* **18**, 265403 (2007).
- ³⁴J. I. Mizobata, A. Fujii, S. Kurokawa, and A. Sakai, *Phys. Rev. B* **68**, 155428 (2003).
- ³⁵A. I. Yanson and J. M. van Ruitenbeek, *Phys. Rev. Lett.* **79**, 2157 (1997).
- ³⁶We used aluminum wire of 125 μm diameter, “temper as drawn,” 99.99%+, Goodfellow Corp., annealed in high vacuum at 350 °C for 72 h.
- ³⁷Aluminum wire, 125 μm diameter, “temper hard,” 99.99%, Advent Research Materials Ltd., Catalogue No. AL500111.